River Flow 2012 – Murillo (Ed.)
© 2012 Taylor & Francis Group, London, ISBN 978-0-415-62129-8

Bend scour reduction induced by an air-bubble screen under live-bed conditions

V. Dugué & A.J. Schleiss
Ecole Polytechnique Fédérale de Lausanne (EPFL), Laboratory of Hydraulic Constructions (LCH), Lausanne, Switzerland

K. Blanckaert
State Key Laboratory of Urban and Regional Ecology, Research Center for Eco-Environmental Sciences (RCEES), Chinese Academy of Sciences (CAS) Beijing, China
Ecole Polytechnique Fédérale de Lausanne (EPFL), Laboratory of Hydraulic Constructions (LCH), Lausanne, Switzerland

ABSTRACT: Open-channel bends are characterized by complex interactions between streamwise flow, curvature-induced secondary flow and bed morphology. These bend effects cause erosion near the outer bank, and deposition near the inner bank. Previous laboratory experiments in a sharply curved flume with a mobile bed under clear-water scour conditions have shown that an air-bubble screen generated with a porous tube on the bed can counteract the curvature-induced secondary flow and lead to a shift of the maximum scour away from the outer bank. The here reported study provides experimental results on the optimization of the bubble screen under live-bed conditions. The air-bubble screen considerably reduces erosion near the outer bank for all investigated configurations of the bubble screen. Comparison of three different locations of the porous tube shows that the bubble screen is most efficient when placed very near to the outer bank.

1 INTRODUCTION

Meanders and open-channel bends are characterized by a typical bed morphology which can be attributed to complex interactions between the streamwise flow of the river, the curvature-induced secondary flow of the bend and the bed morphology (Rozovskii 1957, Struiksma et al. 1985, Blanckaert & Graf 2001, Blanckaert 2010). In the resulting so-called bar-pool bed topography, a point bar develops at the inner bank whereas scour develops in the outer part of the bend. Consequently, constructions located near the outer bank can be endangered, and deposition at the inner bank can reduce considerably the navigable width of the river.

Several countermeasures, including riprap (Martin-Vide et al. 2010), bottom vanes (Odgaard & Kennedy 1983) and outer bank footing (Roca et al. 2009) have already been tested experimentally to counteract bend scour and to obtain a more regular topography. All of these methods have obtained good results, but involved fixed and permanent constructions in the river that can represent a threat for navigation.

An innovative way to manipulate the curvature-induced secondary flow, involving an air-bubble screen, has been tested at LCH-EPFL under different conditions of flow and sediment transport. The bubble screen generates upwards velocities and surface currents, producing two secondary flow cells (Fig. 1). By placing strategically the bubble screen in the river, velocities and boundary shear stresses can be redistributed, leading to morphological modifications. Figure 1 illustrates schematically the working principle of the bubble screen technique and secondary flows involved.

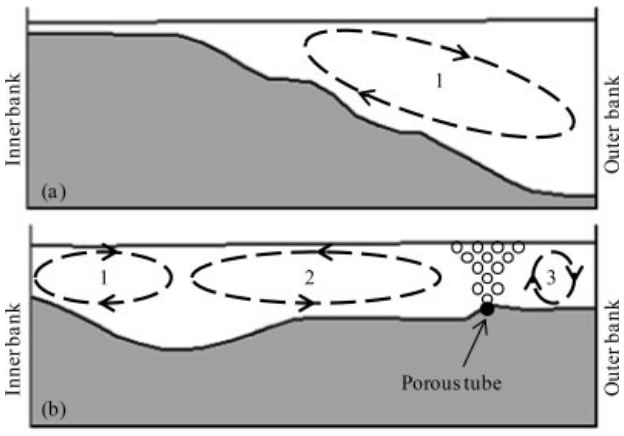

Figure 1. Conceptual sketch of (a) reference case without bubble screen, and (b) case with bubble screen (downstream view). Secondary flow cells are indicated on the Figure. 1, 2, 3 represent the curvature-induced secondary flow, the inner bubble-induced secondary flow and the outer bubble-induced secondary flow, respectively.

Bubble screens have already been used in several hydraulic applications for lake destratification (Wüest et al. 1992), as pneumatic barriers to reduce saltwater intrusion (Nakai & Arita 2002), or to prevent shoaling of navigation channels (Chapman & Scott-Douglas 2002). However, air-bubble plumes and screens have never been applied for morphodynamic purposes. Compared to existing countermeasures, they have the advantages of being non-permanent and to have a favorable ecological impact on the river (oxygenation).

Previous laboratory experiments in a sharply curved channel on a fixed horizontal bottom have shown that a bubble screen placed near the outer bank results in a bubble-induced secondary flow that weakens the curvature-induced secondary flow and shifts it away from the outer bank (Blanckaert et al. 2008). Experiments performed in the same laboratory flume but with a mobile bed under clear-water scour conditions have investigated the influence of the bubble screen on the morphology (Dugué et al. 2011). The scour hole no longer occurred at the outer bank but had been shifted near the inner bank and its depth had been reduced by about 50%.

The objective of the present paper is to continue the investigation of the bubble screen effect by reproducing similar experiments on a mobile bed but under live-bed conditions with constant sediment feeding. The present paper reports experiments without the bubble screen (reference experiment) and with three different positions of the bubble screen. Morphologic comparisons between clear-water scour and live-bed experiments are provided in this paper with the aim to answer the following questions:

Is the bubble screen still efficient under live-bed conditions?

What is its impact on the bend morphology and on mesoscopic bed features?

Which optimized position of the bubble screen has the most beneficial impact on the morphology?

The laboratory flume and the experimental conditions are briefly described. Then, the impact of the bubble screen on the general morphology and on the specific mesoscopic features of the bend under clear-water scour and live-bed conditions is discussed. Finally, the effect of the transverse position of the bubble screen in the bend is discussed.

2 EXPERIMENTS

2.1 *Experimental set-up and instrumental devices*

Laboratory experiments have been performed in a sharply curved flume of constant width $B = 1.3$ m (Fig. 2) with smooth vertical banks. The flume is composed of a 9 m long straight reach, followed by a 193° bend with a centerline radius of curvature of $R = 1.7$ m, and ended by a 5 m long downstream straight reach. A detailed description of the flume is reported in Blanckaert (2002).

A curvilinear reference system (s, n, z) is adopted where s represents the streamwise direction, the transverse n axis points in the outward direction and the vertical z axis in the upward direction.

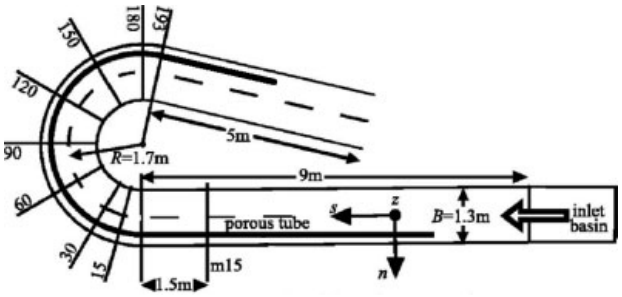

Figure 2. Plan view of the curved channel with the porous tube.

The sediment used for the experiment is uniform quartz sand with a mean diameter of 2 mm. When conducting experiments under live-bed conditions, sediment is continuously fed into the flume near the entrance at a constant rate, resulting in bed-load transport. At the end of the flume, a settling tank is installed to allow the deposition of the transported sediment.

The bubble screen is generated by means of a porous tube connected at both ends to a pressurized-air system. The porous tube is ballasted by means of a chain to avoid large amplitude movements and buoyancy effects.

The air pressure is controlled by means of a manometer and the air discharge measured by means of a rotameter.

Water surface elevation was measured by means of a point gauge and final bottom elevation measurements were performed on a refined grid by means of a laser distometer (every 5° in the bend and every 5 cm in the transversal direction).

Macroscopic and mesoscopic features, such as the point bar and the dunes, were documented by means of photographs.

2.2 *Experimental parameters*

Main hydraulic and air parameters are summarized in Table 1. For all the tests, the initial condition was a flat bed. Experiments were performed under two different conditions of sediment transport.

Two experiments under clear water scour conditions without bubble screen generation (M57_14_00) and with bubble screen generation (MB55_14_p5_d20) were performed until the equilibrium had been reached. Clear water scour conditions were determined based on the critical dimensionless Shields parameter, τ_c, which is approximately 0.04 according to Shields diagram (Breusers & Raudkivi 1991). The dimensionless Shields parameter τ in the upstream straight reach was smaller than its critical value. Hydrodynamics and morphodynamics results have been described in Dugué et al. (2011).

Four short-term experiments were performed with a similar discharge and the same sediment under live-bed conditions with constant sediment feeding ($q_s = 0.025$ kg/(m.s)).

Table 1. Experimental conditions.

Label	Q [l/s]	H_f [m]	U_f [m/s]	Fr_f [-]	P [kPa]	d_b [m]	R/B [−]	R/H_f [−]	B/H_f [−]
M57_14_00	57	0.143	0.31	0.26	–	–	1.3	11.9	9.1
MB55_14_p5_d20	55	0.140	0.31	0.26	500	0.2	1.3	12.2	9.3
M63_10_00	63	0.105	0.46	0.45	–	–	1.3	16.2	12.3
MB63_10_p6_dxx	63	0.105	0.46	0.45	600	0.1, 0.2, 0.3	1.3	16.2	12.3

Q is the water discharge, H_f is the final flume-averaged flow depth, U_f is the final flume-averaged velocity, Fr_f is the final flume-averaged Froude number and d_b is the distance between the porous tube and the outer bank. Experiments are labeled by the bed configuration (M = mobile bed, MB = mobile bed with bubble screen), the discharge [L/s], the water depth [cm], the air pressure [bar] and the distance between the porous tube and the outer bank [cm].

A steepening of the longitudinal slope provided the increase in sediment transport capacity required to transfer the fed sediment through the bend. The increased bed slope led to a decrease in flow depth and an increase in velocities.

The equilibrium morphology in our experiments was obtained after 3 weeks under clear-water scour conditions. In previous long-term experiments under live-bed conditions in the same flume, morphological evolution of the bend was found to be asymptotic and the morphology after 7 h was strongly similar to the equilibrium configuration. This difference in morphologic development between clear-water scour and live-bed conditions is in agreement with observations by Roca et al. (2007). Therefore and to limit the test duration, the short-term experiments were stopped after 7 hours, and the flume was drained to allow the bottom elevation measurements.

The two reference experiments M57_14_00 and M63_10_00 were performed without the bubble screen. Under clear water scour condition, the porous tube was placed at 0.2 m from the outer bank and started 5 m before the bend entry. Under live-bed conditions, three different positions of the porous tube have been tested, with distances from the outer bank of $d_1 = 0.1$ m, d_2=0.2 m and $d_3 = 0.3$ m, respectively. For the MB63_10_p6_d20 experiment, the bubble screen starts in the upstream straight part 5 m before the entry of the bend. In the two others bubble-screen experiments, the porous tube only starts at the entry of the bend.

3 RESULTS

3.1 *Influence of the live-bed condition on the bubble screen efficiency*

Figure 3 illustrates in detail the final bed morphology for the clear water scour experiments without the bubble screen (Fig. 3a), with the bubble screen (Fig. 3b) and the bed configuration after 7 h of run under live-bed conditions without the bubble screen (Fig. 3c) and with the bubble screen (Fig. 3d) The bed reference for each experiment ($z = 0$ m) coincides with the flume-averaged bed level.

In the reference experiments M57_14_00 and M63_10_00, a bar-pool bend topography that is typical of open-channel bends develops, as observed in the literature (Whiting & Dietrich 1993, Roca et al. 2009, Blanckaert 2010). A scour hole appears in the first part of the bend between 60° and 90° and sedimentation occurs near the inner bank, resulting in the formation of a point-bar. A second scour hole with a comparable depth is located at the bend exit. The existence of these two scour holes is related to the sudden change of curvature at the entry and the exit of the bend and the different mechanisms involved are further described in the discussion.

Results of M57_14_00 (Fig. 3a) and M63_10_00 (Fig. 3c) led to the conclusion that the bed topography in reference tests with and without sediment feeding are not significantly different. The main difference is the migration of mobile bed forms under live-bed conditions. However, they do not affect significantly the large-scale bar-pool bend topography.

The bubble screen modified dramatically the morphology under clear-water scour conditions (Fig. 3b). The maximum bend scour between 60° and 90° was shifted away from the outer bank towards the center of the flume and its depth was reduced by about 50%. The bed level was in general much flatter than in the reference experiment. The second scour hole located at the bend exit totally disappeared.

Under live-bed conditions, the bubble screen technique was less efficient to reduce bend scour. The main scour hole located between 60° and 90° still developed, but its spatial extent and its maximal depth were reduced by the bubble screen. The second scour hole at the exit of the bend totally disappeared (Figs 3b, d).

Figure 4 provides visualization of the mesoscopic bedform features in the downstream part of the bend for the four experiments. These bedforms occurred in all experiments. In the reference experiments (Figs 4a, c), large amplitude dunes can be observed. In the bubble screen experiment (Figs 4b, d), dunes had a smaller wavelength and amplitude. In the M55_14_p5_d20 experiment, their location has been shifted in the inwards direction, indicating that the core of maximum streamwise velocities is no longer near the outer bank. Under live bed conditions, dunes are covering the entire cross-section and are migrating on top of

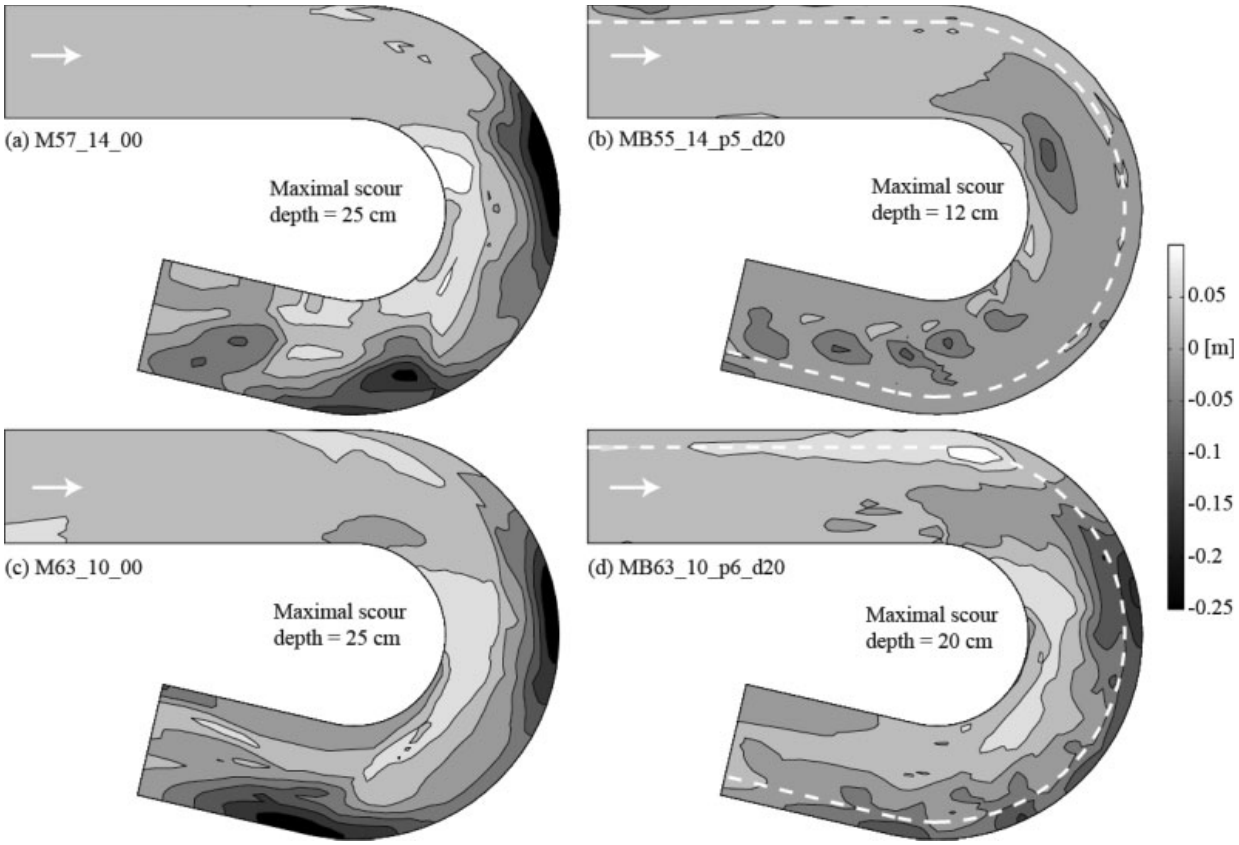

Figure 3. Isolines of the bed elevation with an interval of 0.05 m derived from laser altimetry measurements for the experiments under clear-water scour conditions without bubble screen M57_14_00 (a) and with bubble screen MB55_14_p5_d20 (b) and for the experiments under live-bed conditions without bubble screen M63_10_00 (c) and with bubble screen MB63_10_p6_d20 (d). The same gray scale has been used to facilitate comparison. The location of the porous tube is indicated with a white dashed line in the bubble experiment. The reference ($z = 0$ m) corresponds to the flume-averaged bed level.

the porous tube. Their shapes reveal that the maximum streamwise velocities are further outwards as compared to the clear-water scour experiments.

In addition, some ripples, evolving on the top of the porous tube in the inwards direction and parallel to the axis of the porous tube, have also been observed, indicating the local effect of the bubble screen.

3.2 *Impact of the location of the bubble screen*

The transversal location of the bubble screen is assumed to have an important effect on the bend morphology and is investigated by varying the distance between the porous tube and the outer bank.

Figure 5 provides the detailed final bed topography of M63_10_p6_d10 and M63_10_p6_d30 experiments in which two different transversal positions of the porous tube, respectively 0.1 m and 0.3 m from the outer bank, have been investigated under live-bed conditions. These results can be compared to the reference situation without bubble screen (Fig. 3c) and to the M63_10_p6_d20 experiment where the porous tube was located at 0.2 m from the outer bank (Fig. 3d).

In the three bubble-screen experiments, the first scour hole located between 60° and 90° still exists but its spatial extent and its maximal depth have been reduced whereas the second pool located at the exit of the bend does not appear anymore.

In the MB63_10_p6_d10 and MB63_10_p6_d20 experiments, the area covered by the first scour hole is reduced and the maximal depth is decreased by 8 and 5 cm, respectively, as compared to the reference experiment. In the MB63_10_p6_d30, the area covered by the first scour hole is not modified by the bubble screen. The point bar's spatial extent has decreased when using the bubble screen especially when the porous tube is located at 10 cm (Fig. 5a) or 20 cm (Fig. 3d) from the outer bank. These results suggest that the bubble screen is more efficient when located the nearest to the outer bank.

The streamwise evolution of the transverse bed slope (determined by linear fitting) in the four experiments is drawn in Figure 6a. It illustrates well the scour distribution around the whole flume. In the reference experiment, the transversal slope indicates two main scour locations at 85° and 190° as observed in Figures 3 and 5. For the three bubble screen experiments, the transversal slope is strongly reduced at the end of the bend and slightly reduced in the first scour hole. The transverse bed slope also shows less large-scale variation around the bend. Smaller scale oscillations due to migrating dunes are amplified in the bubble-screen experiments.

Cross-sections of the bed topography for the four experiments are compared at 90° and 180° where the most important scour holes are located (Figs 6b, c).

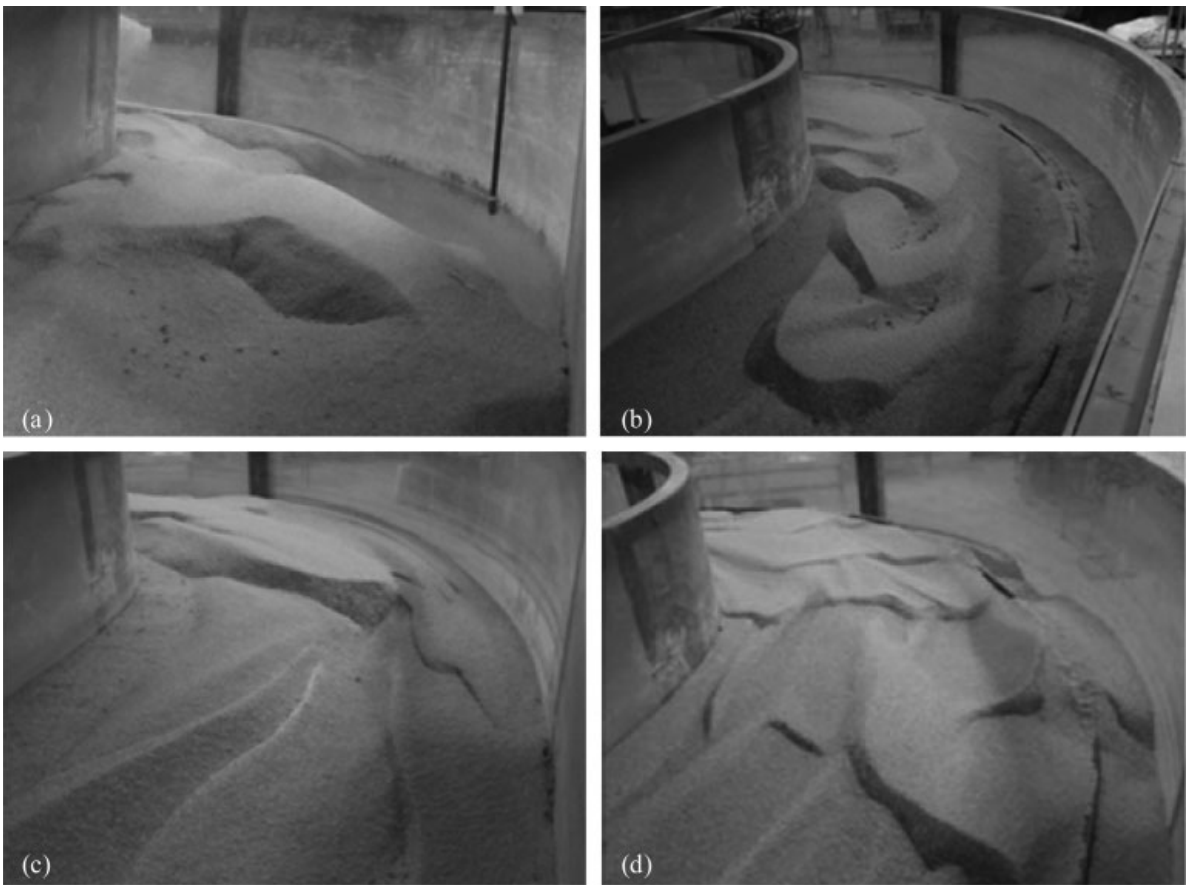

Figure 4. Visualization of the mesoscopic bedform features in the downstream part of the bend (between 120° and the bend exit at 193°) for the experiments M57_14_00 (a), MB55_14_p5_d20 (b), M63_10_00 (c) and MB63_10_p6_d20 (d).

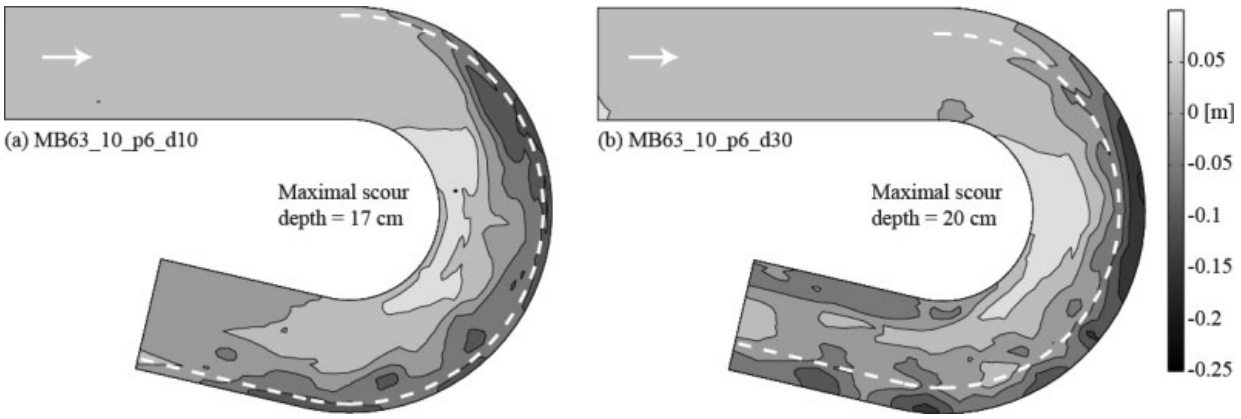

Figure 5. Isolines of the bed elevation with an interval of 0.05 m derived from laser altimetry measurements for the MB63_10_p6_d10 (a) and MB63_10_p6_d30 experiments (b) with the porous tube placed respectively at 0.1 and 0.3 m from the outer bank under live-bed conditions. The same gray scale as Figure 3 has been used to facilitate comparison.

In the 90° cross- section (Fig. 6b), the scour reduction and the elevation of the point bar is weaker than in the 180° cross-section where it has been reduced by more than 50% for the MB63_10_p6_d20 test.

For all configurations, dunes superimposed to the macroscopic bed features and migrating in the downstream direction are observed. In the reference M63_10_00 experiment, the largest dune with an amplitude of 10 cm is located in the center of the channel, as observed under clear-water scour conditions (Fig. 4a). Smaller dunes with amplitudes of 2 to 5 cm superimposed on the largest dune are migrating around the bend. In all the bubble screen experiments, maximal dune amplitudes seem to decrease. For each location of the air-bubble screen a different mesoscopic configuration has been observed, showing the influence of the location of the bubble-screen induced secondary flow on the local morphology.

4 DISCUSSION

The reported experiments clearly reveal that the bend morphology as well as the evolution and general aspect

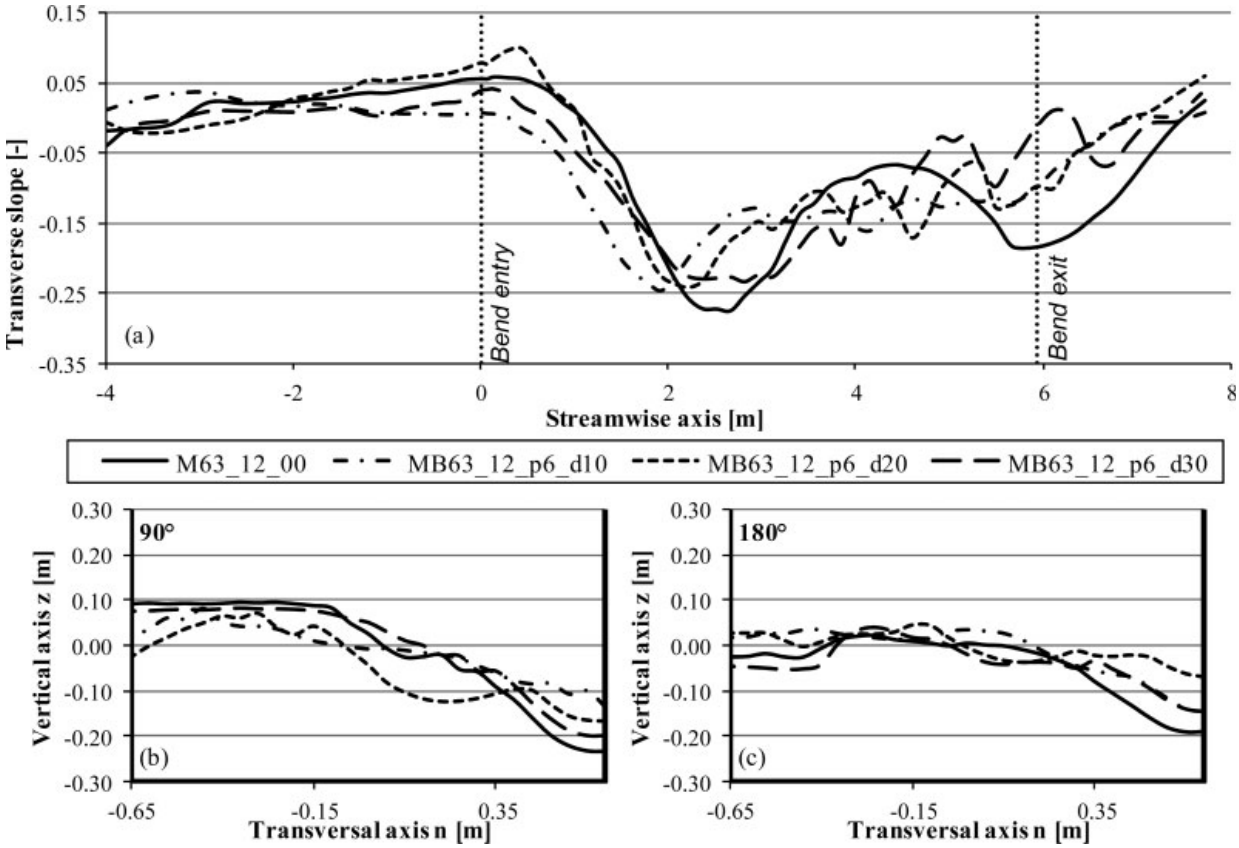

Figure 6. Comparison of the reference M63_10_00 experiment without the bubble screen and MB63_10_p6_d10, MB63_10_p6_d20, MB63_10_p6_d30 experiments with the bubble screen at different locations, (a) Streamwise evolution of the transverse bed slope around the flume and bed elevations in the cross-sections at 90° (b) and 180° (c) in the bend.

of mesoscopic bedforms can be modified by the implementation of a bubble screen near the outer bank. However, some comments need to be addressed.

Bend morphology obtained under clear-water scour conditions was found to be strongly modified by the use of the bubble screen whereas under live-bed conditions, the bubble screen was less efficient in reducing scour, especially at the bend entry. This difference of the bubble screen efficiency can be explained by different factors:

To obtain live-bed conditions, the mean water velocity was increased through an increase in streamwise bed slope and a lowering of the water depth. These two modifications can have a significant impact on the efficiency of the bubble screen.

First, the smaller water depth has a negative impact on the development and strength of the bubble-induced secondary flow cell, which is strongly dependant of the aspect ratio H/B(Riess & Fanneløp 1998).

Second, the increase of the mean velocity strengthens the two mechanisms involved in the development of the two scour holes.

The first and more pronounced scour hole, located between 60° and 90° is induced by the impingement of the upstream straight flow on the outer bank and by the resulting abrupt reversal of flow near the bed (Whiting & Dietrich 1993, Ferguson et al. 2003, Blanckaert 2010). As seen in Frothingham & Rhoads (2003), an increase of the mean streamwise velocity strengthens the flow that collides with the bank, resulting in stronger downward velocities impinging on the bed. Consequently, under live-bed conditions, the bubble-induced secondary flow is too weak to prevent this inertia induced flow impingement and can therefore only slightly reduce the scour depth in this first scour hole.

In the second part of the bend, as the curvature is strongly decreasing, the still dominant curvature-induced secondary flow advects the core of maximum streamwise velocities near the base of the outer bank, where it promotes the development of the second scour hole (Frothingham & Rhoads 2003, Blanckaert 2010). Under both sediment conditions, the bubble-induced secondary flow is able to modify considerably the morphodynamics and to attenuate the effects due to the sudden disappearance of the curvature at the bend exit. This effect is more pronounced under clear-water scour conditions as dunes only appears in the center part of the flume. In live-bed conditions, the scour hole is avoided but dunes are still covering the whole cross-section.

Obviously, the reduction of scour obtained in the studied laboratory configuration with the bubble screen is indicative, as it is strongly dependant of the geometry of the river, the sediment characteristics and finally the bend curvature.

5 CONCLUSIONS

Experiments under live-bed conditions have been performed with and without a bubble screen, in a sharply curved flume. The experimental results show that the bubble screen significantly modifies the morphology and reduces the bend scour near the outer bank. If the first scour hole located at the entry of the bend cannot be completely avoided, the second pool located at the exit of the bend is strongly reduced whatever the bubble screen location is.

Different locations of the bubble screen have been tested. The optimal position was found to be very near the outer bank.

A better understanding of the redistribution of the velocity field induced by the counter-rotating bubble-induced cell is relevant and is under investigation.

ACKNOWLEDGEMENT

This research was financially supported by the Swiss National Science Foundation under grants 200021-125095. The second author was partially funded by the Chinese Academy of Sciences fellowship for young international scientists under Grant No. 2009YA1-2 and by the Sino-Swiss science and technology cooperation for the joint research project GJH20908.

REFERENCES

Blanckaert, K. & Graf, W. H. 2001. Mean flow and turbulence in open-channel bend. *Journal of Hydraulic Engineering* 127(10): 835–847.

Blanckaert, K. 2002. Flow and turbulence in sharp open-channel bends. PhD thesis 2545, Ecole Polytechnique Fédérale de Lausanne, Switzerland.

Blanckaert, K., Buschman, F. A., Schielen, R. & Wijbenga, J. H. A. 2008. Redistribution of velocity and bed-shear stress in straight and curved open-channels by means of a bubble screen: Laboratory experiments. *Journal of Hydraulic Engineering-ASCE* 134(2): 184–195.

Blanckaert, K. 2010. Topographic steering, flow recirculation, velocity distribution, and bed topography in sharp meander bends. *Water Resources Research* 46, W09506, doi:10.1029/2009WR008303.

Breusers, H. N. C. & Raudkivi, A. J. 1991. *Scouring*. International Association for Hydraulic Research, ed., Bakelma, Rotterdam, The Netherlands.

Chapman, J. E. & Scott-Douglass, L. 2002. Evaluation of a berth sedimentation control technology in the Kill Van Kull: The AirGuard pneumatic barrier system. *Proc. of the third Specialty Conference on Dredging and dredged material disposal*, Orlando, USA.

Dugué, V., Blanckaert, K. & Schleiss, A. J. 2011. Influencing bend morphodynamics by means of an air-bubble screen – Topography and velocity field. *Proc. of the 7th IAHR Symp. on River Coastal and Estuarine Morphodynamics*, Beijing, China.

Ferguson, R. I., Parsons, D. R., Lane, S. N. & Hardy, R. J. 2003. Flow in meander bends with recirculation at the inner bank.*Water Resources Research* 39(11):1322.

Frothingham, K. M. & Rhoads, B. L. 2003. Three-dimensional flow structure and channel change in an asymmetrical compound meander loop, Embarras river, Illinois. *Earth Surface Processes and Landforms* 28(6): 625–644.

Nakai, M. & Arita, M. 2002. An experimental study on prevention of saline wedge intrusion by an air curtain in rivers. *Journal of Hydraulic Research* 40(3): 333–339.

Martin-Vide, J. P., Roca, M. & Alvarado-Ancieta, C. A. 2010. Bend scour protection using riprap. *Proc. of the Institution of Civil Engineers-Water Management* 163(10): 489–497.

Odgaard, A. J. & Kennedy, J. F. 1983. River-bend bank protection by submerged vanes. *Journal of Hydraulic Engineering-ASCE* 109(8): 1161–1173.

Roca, M., Martin-Vide, J. P. & Blanckaert, K. 2007. Reduction of bend scour by an outer bank footing: Footing design and bed topography. *Journal of Hydraulic Engineering-ASCE* 133(2): 139–147.

Roca, M., Blanckaert, K. & Martin-Vide, J. P. 2009. Reduction of bend scour by an outer bank footing: Flow field and turbulence. *Journal of Hydraulic Engineering-ASCE* 135(5): 361–368.

Struiksma, N., Olesen, K. W., Flokstra, C. & de Vriend, H. J. 1985. Bed deformation in curved alluvial channels. *Journal of Hydraulic Research* 23(1): 3605–3614.

Riess, I. R. & Fanneløp, T. K. 1998. Recirculating flow generated by line-source bubble plumes. *Journal of Hydraulic Engineering-ASCE* 124(9): 932–940.

Rozovskii, I. L. 1957. Flow and water in bends of open channels. *Academy of Sciences of the Ukrainian SSr, Isr. Progr. Sc. Transl.,* Jerusalem, Israel.

Whiting, P. J. & Dietrich, W. E. 1993. Experimental studies of bed topography and flow patterns in large-amplitude meanders. 1. Observations. *Water Resources Research* 29(11): 3605–3614.

Wüest, A., Brooks, N. H. & Imboden, D. M. 1992. Bubble plume modeling for lake restoration. *Water Resources Research* 28(12): 3235–3250.